

Fuel and Time Optimize and Adaptive Control for Gravity Gradient Spacecraft

A. P. Nagwai, M. O. Akinwande and Samson. Agboola*

Department of Statistics, Ahmadu Bello University Zaria, Nigeria

Received: 12 Feb. 2017, Revised: 2 Mar. 2017, Accepted: 17 Mar. 2017

Published online: 1 May 2017

Abstract: This paper treats the time/fuel optimal control of gravity gradient spacecraft. The equations of motion of the spacecraft are simplified such that the maximum principle becomes applicable: the validity of this approximation is proven by comparison of the simulation results of the rigorous and the simplified system. Based upon the simplified equation, a time/fuel optimal law for space craft attitude control is developed. This law is based upon definition of a fuel savings angle, a new way of defining the trade-off between pure time optimality and pure fuel optimality. Chattering in the vicinity of zero angles and zero rates is limited by a simple adaptive modification.

Keywords: Spacecraft, Optimize, Maximum principle, Time and Fuel

SYMBOLS

The index i stands for yaw ($i=x$), roll ($i=y$) and pitch ($i=z$) and is omitted when no distinction in the treatment of the different axes is necessary.

a_j = gravity gradient coefficients, $j= x,y,z$

I_{ii} = moments of inertia, $i= x,y,z$

r = distance from earth center to spacecraft center

T_{ci} = control torque, $i= x,y,z$

T_{di} = disturbance torque, $i=x,y,z$

r_+ = line for switching from $u = 0$ to $u = +k$

r_- = line for switching from $u = 0$ to $u = -k$

$_-$ = line for switching from $u = k$ to $u = 0$

$_+$ = line for switching from $u = -k$ to $u = 0$

μ = earth gravitational constant

$\omega_{0=}$ orbital angular rate for circular equilateral orbit

All other variables are defined wherever needed in the text.

1 Introduction

Several spacecraft applications and experiments, e.g , laser communications and some types of earth observation, make a precision of 001^0 . Furthermore, severe constraints on the amount of fuel available in spacecraft make it necessary to develop economical policies for attitude control. A promising approach is to combine active control (e.g , by means of electric

propulsion devices) and passive (gravity gradient) control 7. The configuration and the equations of motion of gravity gradient spacecraft (in the case considered here, a synchronous earth satellite) will be presented in the following.

Sengupta and Vadali (2005) present an orbit transfer/formation control algorithm for an Earth orbiting spacecraft. Their approach employs Lyapunov analysis with Euler parameters to characterize the orbit.

Vaddi *et al.*, (2005) develop a control strategy for a two spacecraft formation orbiting a central body. The strategy utilizes orbital element difference s . Analysis shows the solution is fuel-optimal and maintains homogenous fuel consumption between spacecraft. Their results correlate with similar numerical optimization studies.

Richard (2006) investigates Nonlinear Control Design Techniques for Precision Formation Flying at Lagrange Points where he examines the precision formation flying control architecture, characterizing the relative performance of linear and nonlinear controllers. By minimize the influence of design parameters in the comparison, analysis employs same controller gains, and incorporates an integrator in the linear control design. Simulation architecture includes a full gravitational model and solar pressure effects were included while the Spacecraft model properties are based on realistic mission design parameters. The Nonlinear controllers are

* Corresponding author e-mail: abuagboola@gmail.com

developed based on Lyapunov analysis, including both non-adaptive and adaptive designs. While the linear controller demonstrates greater robustness to model uncertainty, both nonlinear controllers exhibit superior performance.

Scott Y (2013) on his thesis work on simulation of spacecraft damage tolerance and adaptive controls where he expands on the topic, discussion on the application of adaptive controls to spacecraft and simulating a possible damage tolerant control implementation designed for rapid changes in inertia by The developing of adaptive controls and enabling technology for them to reached a point where new and innovative uses are now becoming possible. Also by introducing a modified adaptive PID (Proportional Integral Derivative) controller with adaptive feed forward control to this simulated spacecraft, it is demonstrated that the controls have achieved significant damage tolerance.

2 Configuration and Equation of Motion

The satellite under consideration is shown in figure1. The control problem consists in bringing the attitude angles of the spacecraft to zero. The attitude angles are defined as the Euler angles between the x_b, y_b, z_b – system and the Attitude coordinates system (x_o, y_o, z_o). The axes of the letter are defined by the following directions:

x_o pointing from the earth center of mass to the spacecraft center of mass

y_o normal to x_o , in the orbit plane and in the same sense as the vehicle motion

z_o normal to the orbit plane and such that (x_o, y_o, z_o) constitutes a right handed orthogonal coordinate system

Figure 2 shows both coordinate systems mentioned and the Euler angles used.

According to standard definitions, and considering figure 2, we have:

Pitch α about z_o

Roll about $-y^1$

yaw ψ about x_b

The following equations of motion are valid for this satellite:

$$[I] \begin{pmatrix} x_b \\ y_b \\ z_b \end{pmatrix} = \begin{pmatrix} \delta_{xb} \\ \delta_{yb} \\ \delta_{zb} \end{pmatrix} \quad (1)$$

where

$$\delta_{xb} = M_{xb} + M_{xd} \sin \rho_2 + M_{zd} \cos \rho_2 - (y_b H_{zb} - z_b H_{yb}) - P \cos \rho_2 + T_{cx} + T_{dx}$$

$$\delta_{yb} = M_{yb} + M_{xd} \cos \rho_2 \cos \rho_1 + M_{SD} \sin \rho_1 - M_{zd} \sin \rho_2 \cos \rho_1 - (z_b H_{xb} - x_b H_{zb}) \quad (2)$$

$$+ P \sin \rho_2 \cos \rho_1 + T_{cy} + T_{dy}$$

and,

$$\delta_{zb} = M_{zb} + M_{xd} \cos \rho_2 \sin \rho_1 + M_{SD} \cos \rho_1 - M_{zd} \sin \rho_2 \sin \rho_1 - (x_b H_{yb} - y_b H_{xb})$$

$$+ P \sin \rho_2 \sin \rho_1 + T_{cz} + T_{dz}$$

The torque M_{ib} and M_{id} are caused by the gravity gradient effect (Zach F., 1970)

Also, P and M_{SD} and the equation of motion for the damper rod and the relationship between the time derivatives of the Euler angles and the $i_b (i= x,y,z)$ (Zach F., 1970)

A digital program was written which allows the simulation of the satellite motion according to the simulation of the motion presented.

3 Small Angle Approximation of the Equations of Motion

It is shown in that for small angles and negligible inner damping, the equations of motion can be approximated by:

$$(\text{yaw}) + \omega_0^2 \frac{I_{zz} - I_{yy}}{I_{xx}} \psi - \frac{I_{zz} - I_{yy} - I_{xx}}{I_{xx}} \omega_0 \dot{\psi} = \frac{T_{cx} + T_{dx}}{I_{xx}} \quad (3)$$

$$(\text{roll}) + 4 \omega_0^2 \frac{I_{zz} - I_{xx}}{I_{yy}} \psi - \frac{I_{zz} - I_{xx} - I_{yy}}{I_{yy}} \omega_0 \dot{\psi} = \frac{T_{cy} + T_{dy}}{I_{yy}} \quad (4)$$

and

$$(\text{pitch}) \ddot{\alpha} + 3 \omega_0^2 \frac{I_{zz} - I_{xx}}{I_{yy}} \alpha = \frac{T_{cz} + T_{dz}}{I_{zz}} \quad (5)$$

It is now assumed that

$$I_{zz} \approx I_{yy} + I_{xx} \quad (6)$$

As is true, e.g., for the ATS-D and ATS-E spacecraft.

Thus, Equations 3-5 become

$$\Psi + a_\psi \Psi = u_\psi + d_\psi \quad (7)$$

$$+ a_\gamma \dot{\gamma} = u_\gamma + d_\gamma \quad (8) \text{ and}$$

$$\ddot{\alpha} + a_\alpha \dot{\alpha} = u_\alpha + d_\alpha \quad (9)$$

where the a_i, u_i , and d_i can be gain immediately by comparison with Equations 3-5. (Zach F. and Frick R.H.,)

When $d = d = d_\alpha = 0$ and u_ψ, u, u_α are constant each of the equation 7-9 gives circles for each of the phase plane plots ($\psi, \dot{\psi}/va_\psi$), ($\gamma, \dot{\gamma}/va_\gamma$), ($\alpha, \dot{\alpha}/va_\alpha$) respectively.

Simulations of the GGS under the same conditions result in circles for the phase plane plots (trajectories) for angles up to 10° . This, together with the result of (Zach F., 1970), proves the applicability of the approximations used.

Zach F (1970) treated the case of coupled satellite axes is. However, no unique switching lines in the angle angular rate phase can be derived.

4 Derivation of the Time/Fuel Optimal Control Law.

The maximum principle 4,5 will be applied to derive the time/fuel optimal control for $\dot{x} = u$ in order to drive x and \dot{x} to zero, where x stands for ψ, γ, α of Eqs. 7 and 9.

The performance index is given by

$$P = \int_{t_0}^{t_e} (\lambda_e + \lambda_f |u|) dt \quad (10)$$

Where t is the start and t_e the end of control action. λ_f the fuel weighting factor.

E.g, $\lambda_f = 0$ leads to a pure time optimal solution. The Hamiltonian 5 for this case is with $x = x_1$ and $x_2 = \dot{x}_1$.

$$H = p_1 x_2 + p_2 (u - a x_1) - \lambda_t - \lambda_f |u| \quad (11)$$

H is maximized at every instant of time by

$$u = k \operatorname{sgn} p_2 \text{ for } |p_2| = \lambda_f \quad (12)$$

and

$$u = 0 \text{ for } |p_2| < \lambda_f \quad (13)$$

With Equation 11 and $dp_i/dt = -\partial H/\partial x_i$ (see Reference5), one obtains (14)

$$P_2 = P_m \sin(a^{1/2}t + \varphi) \quad (15)$$

where P_m and φ are integration constants.

The final arc: Figure 3 shows p_2 and u versus time t . From this figure it can be said that u has to be on at the final time t_c ; this is true since the state would never reach the origin as center. The on time before reaching the origin is between 0 and t_c , t_c being the maximum on time. Therefore the part of the trajectory which leads the state to the origin has to be part of a semicircle with its center at $+k/a$ or $-k/a$ as shown in figure 2. The longest arc leading to the origin is given by $\beta = \omega t_c$, where $\omega = a^{1/2}$

Coasting before final arc: From Figure3 it is obvious that the state has to have a coasting period reaching this final arc unless the initial condition happened to be on this final arc. The length of the coasting period is limited by $t_{off} = \omega t_{off}$. If the initial conditions are far enough from the origin that more thrust intervals than the final one leading to the origin are required to drive the state to the origin the coasting interval is given by t_{off} . This means that by going back in time by t_{off} the time of switching from control to coasting has been found. In the phase plane this can be depicted by drawing circular arcs with the center in the origin and starting at each point of the arcs of Figure 4. The length of these arcs for coasting is given by t_{off} . The endpoints of these arcs again form circle arcs of Figure 4, by an angle counter clockwise about the origin. This is shown in Figure 5. It can be seen from this Figure that each initial state lying within the hatched area can be brought to the origin in a time-fuel optimal maneuver by coasting to r_+ or r_- , respectively and then by control application.

Thrusting before final coasting period: If the initial state does not lie in the hatched area of the Figure 5 one sees from Figures 3 and 5 that another thrusting period is required with control of the reverse sign when compared with the final control. This thrusting period again can last up to a time interval of t_c . Again shorter intervals than t_c for thrusting's are applicable for cases where the initial condition is located such that it can be brought to Λ_- by thrusting intervals less than t_c . In the general case of thrust application of exactly t_c duration of all possible trajectories for this period again are circular arcs with an angle β and their centers at $-k/a$ or $+k/a$ or \pm/a , respectively. This means that the geometric locus of their starting points can be constructed by rotation of Λ_- or Λ_+ , respectively, in Figure5 counterclockwise by an angle β . The result is shown in figure6.

Complete switching lines: The procedures outlined can be pursued in the same manner as above. The geometric relationship produced by rotating the circle arcs by β or φ , respectively, show that all arcs which form the switching lines have their center on straight lines as shown in Figure7. Also, the intersection points of the arcs lie on a straight line.

The Equations for the switching lines are given in Reference5.

For the case where $\lambda_f=0$ the pure time optimal control law is derived. This means for the switching lines that $\lambda_f=0$ which leads to the well known semicircles as switching lines for the system $\dot{x} + ax = u$ (see Fig.8).

On the other hand, for $\lambda_t=0$ the pure fuel optimal control law is derived. In this case thrusting is only provided when the state is exactly on the $x^2 a^{-1/2}$ -axis, which means an impulse at this time. This corresponds with the results derived in reference, where it is shown that most economic control for a system given by $\dot{x} + ax = u$ is achieved when the thruster is only in operation when the state falls on the $x^2 a^{-1/2}$ -axis.

5 Adaptive Features and Application

The optimal control law derived has been applied to a seven degree of freedom computer simulation for gravity gradient spacecraft. The results show that very good consistency is obtained between this simulation and the simplified plant $\dot{x} + ax = u$. However, this is only valid as long as the distance sq of the state from the origin is

$$sq = \sqrt{x_1^2 + x_2^2} / a = 0.2 \text{ degrees} \quad (16)$$

In many spacecraft attitude control cases, much higher accuracy is required. For such requirements, the nonlinearities and cross-coupling between the different axes becomes crucial.

The application for the optimal control (as derived for the linearized plant model) leads to chattering in the vicinity of the phase plane origin. Two principles can be applied which eliminates such chattering. One is based upon (disturbances) identification, the other, is based on control performance. We only apply the second method here.

6 Adaptive Control Based upon Control Performance

Chattering about the origin is caused by deviations of the trajectory the trajectory of the plant $\dot{x} + ax = u$. These results in missing of the origin (see Figure 9).

Because missing of the origin is more severe when the applied control torque is higher, we developed a control level k based upon the behavior of the trajectory as it approaches the origin or (if overshoot occurs) as it departs from it. We define this behavior as control performance; this type of performance obviously is related to control accuracy.

Our test have shown that the control level adjustment is best achieved by letting (for states approaching the origin)

$$K_{db} = C_1 \frac{sq}{db} k \quad (17)$$

where

$$C_1 = \text{constant}$$

$$sq = \sqrt{x_1^2 + x_2^2} / a$$

and db is a dead band for sq , such that $k_{db} < k$ for $sq < db$ and $k_{db} = k$ for $sq = db$.

This means that this control level adaptation is only applied within a certain dead band. C_1 and db are optimized by experimentation. For states going away from the origin we have found that

$$k_{db} = C_2(sq_{i+1} - sq_i) \cdot k \text{ for } C_2(sq_{i+1} - sq_i) = 1$$

and (18)

$$k_{db} = k \text{ for } C_2(sq_{i+1} - sq_i) = 1$$

Provides very satisfying and stable control performance. In the last equation, sq_i and sq_{i+1} are two distances of the phase of the origin in two subsequent sampling times. (Obviously we assume here that sq_i is measured in discrete time fashion.) C_2 has been optimized by experimentation.

We want emphasize that the combination of the more mathematically derived time-fuel optimal control law and the more empirically found control level adaptation are essential for stable working conditions; this results in much higher pointing accuracy of the S/C (i.e., maintaining the state close to the origin) and high fuel savings when compared to conventional control. In particular, the pointing can be improved from $.0018^\circ$ (in roll) and $.00039^\circ$ (in pitch) to better than 10^{-6} degrees, while fuel expenditure is decreased by a factor of 0.1.

7 Concluding Comments

Time/fuel optimal control procedures have been derived for gravity gradient satellites where yaw and roll axes decoupled. Because it seems to be impossible to derive such control laws for the complete, coupled satellite equation of motion, it is recommended to decouple the yaw and roll axes by proper choice of the satellite moments of inertia. Adaptive features have to be added to the control law to make it applicable for small angles. We want to point out that here, as in many other cases, the definition of optimality is more or less arbitrary. Exact definitions, however, provide a basis for optimal control developments. Control laws gained by purely theoretical methods are usually more sufficient for practical applications, e.g., due to uncertainty in the mathematical model, or in the knowledge of disturbances, or because the mathematical model only could be treated in the approximate form. This requires additional efforts, such as adaptive control, and, most important, extensive experimentation with either the real system or a sufficiently realistic computer simulation. Furthermore, it should be pointed out that optimal control laws, due to their trade-off characteristics, are only of practical importance if they are easy to realize. This seems to postulate a new optimality criterion which takes the simplicity of application and realization into consideration.

Acknowledgement

Part of the work for this paper was accomplished while the author(s) held a National Research Council Postdoctoral Resident Research Associate ship supported by the national Aeronautics and Space Administration, Goddard Space Flight Center. The author(s) is very much obliged to Mr. W. Isley and Mr. D. Enders for their valuable suggestions, as well as to computing and software, Inc., for the support provided during the preparation of this paper.

Appendix

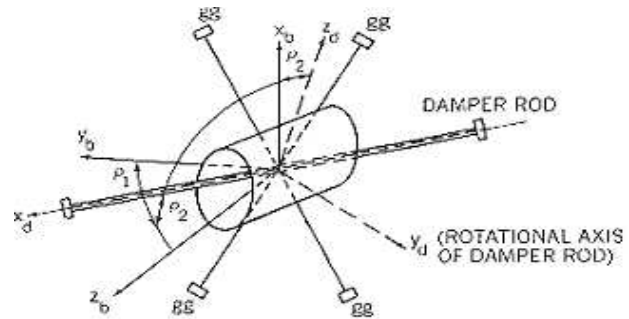


Fig. 1: Gravity Gradient Satellite. X_b and y_b lie in the plane of the four booms and are fixed to the spacecraft, x_d , y_d and z_d are fixed to the damper rod.

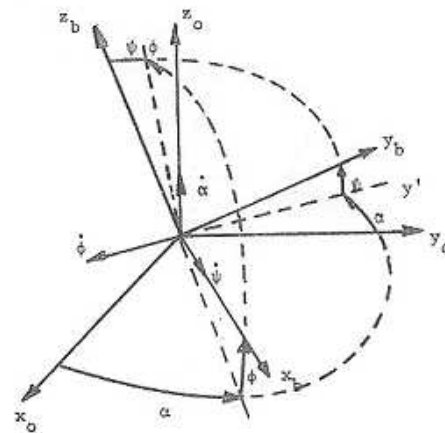


Fig. 2: Body fixed coordinate system and attitude coordinate system.

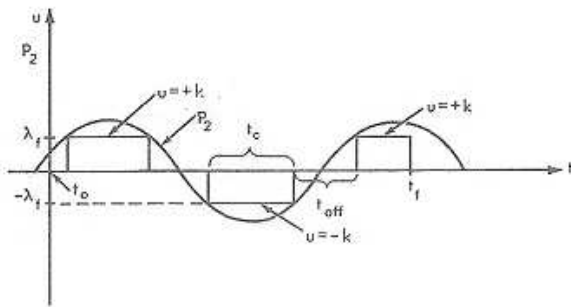


Fig. 3: Control u and auxiliary variable P_2 .

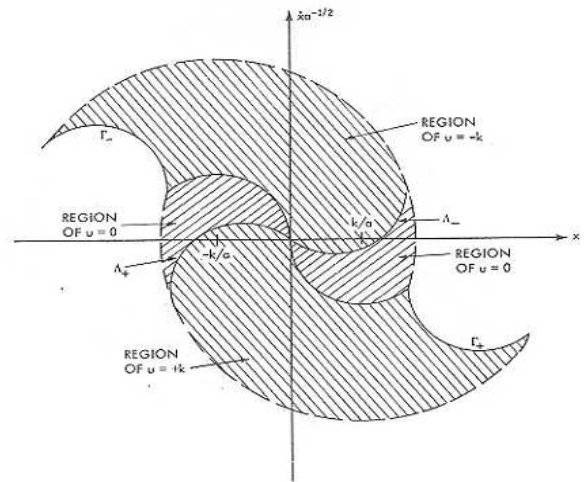


Fig. 6: Extension of Fig. 5, showing regions where $u = +k, 0, -k$ is applied.

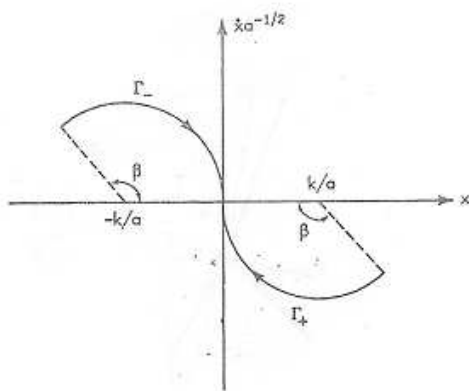


Fig. 4: Final arc.

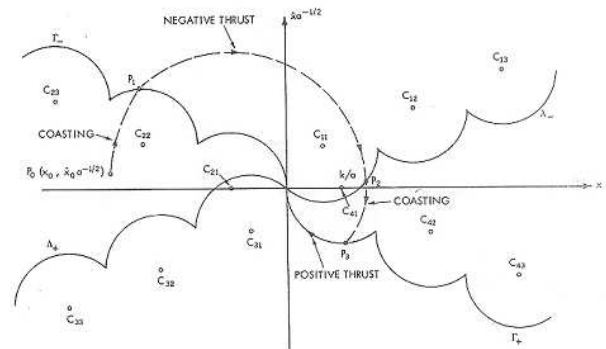


Fig. 7: Switching lines with sample optimal trajectory. $C_{ik} \dots$ centers of switching circle arcs.

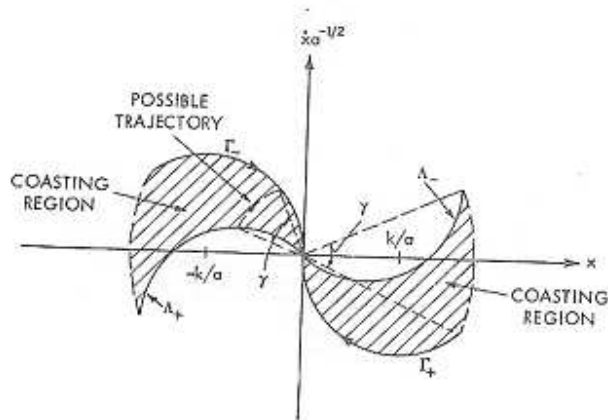


Fig. 5: Coasting regions and switching lines.

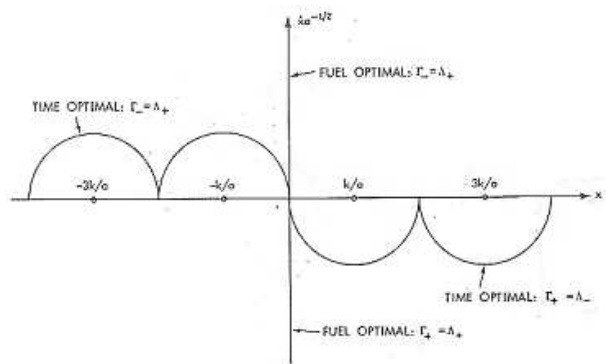


Fig. 8: Reduction of the time/fuel optimal switching lines to pure time optimal case

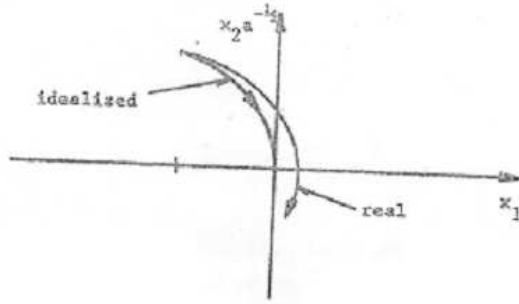


Fig. 9: Behavior of the real and idealized trajectories.

References

- [1] Barrett, C.C.,(1966) "The development of a mathematical model and a study of one method of orbit adjust and station keeping gravity-oriented satellites," *TN D-3652, NASA, Washington, D.C.*,
- [2] Zach F., (1970) "Time optimal control of gravity gradient satellites," *Journal of Spacecraft and Rockets*, 7(2), 1434-1440
- [3] Frick, R.H., (1965) "Perturbation of a gravity gradient stabilization system," *Report AD 623279, the Rand Corp., Santa Monica, California*,
- [4] Zach,F., "Practical optimal control," Springer-Verlag, Wien-New York, in publication.
- [5] Isley, W. (1968) "Optimal control application for electrothermal multijet systems on synchronous earth spacecraft," *Journal of spacecraft and rockets*, vol. 5(12)
- [6] Scott Y. Nakatani (2013) "simulation of spacecraft damage tolerance and adaptive controls" *Thesis Naval Postgraduate School*
- [7] Richard J. Luquette,(2006) "Nonlinear Control Design Techniques For Precision Formation Flying At Lagrange Points" *Dissertation*
- [8] Sengupta P. and Vadali, S. R., (2005) "Satellite Orbit Transfer and Formation Reconfiguration via an Attitude Control Analogy," *Journal of Guidance, Control, and Dynamics*, 28(6), 1200-1209.
- [9] Vaddi S. S., Alfriend K. T., Vadali, S. R. and Sengupta P., (2005) "Formation Establishment and Reconfiguration Using Impulsive Control," *Journal of Guidance, Control, and Dynamics*, 28(2), 262-268.



Ambi Polycarp Nagwai
Professor at Department of Statistics, Ahmadu Bello University Zaria, Nigeria



Akinwande Michael Olusegun B.Sc. Statistics and M.Sc. Statistics- Department of Statistics, Ahmadu Bello University Zaria and Master of Information Management (MIM)- Ahmadu Bello University Zaria, Nigeria



Samson Agboola
B.Sc. Statistics - University of Jos, M.Sc. Statistics - Department of Statistics, Ahmadu Bello University Zaria and Current running Ph.D. Statistics - Department of Statistics, Ahmadu Bello University Zaria, Nigeria